

This is an Open Access document downloaded from ORCA, Cardiff University's institutional repository: <https://orca.cardiff.ac.uk/id/eprint/126293/>

This is the author's version of a work that was submitted to / accepted for publication.

Citation for final published version:

Al Rahal, Okba, Hughes, Colan E., Williams, P. Andrew, Logsdail, Andrew J., Diskin-Posner, Yael and Harris, Kenneth D. M. 2019. Polymorphism of L-tryptophan. *Angewandte Chemie International Edition* 58 (52) , pp. 18788-18792. 10.1002/anie.201908247

Publishers page: <http://dx.doi.org/10.1002/anie.201908247>

Please note:

Changes made as a result of publishing processes such as copy-editing, formatting and page numbers may not be reflected in this version. For the definitive version of this publication, please refer to the published source. You are advised to consult the publisher's version if you wish to cite this paper.

This version is being made available in accordance with publisher policies. See <http://orca.cf.ac.uk/policies.html> for usage policies. Copyright and moral rights for publications made available in ORCA are retained by the copyright holders.



# Polymorphism of L-Tryptophan<sup>‡</sup>

Okba Al Rahal,<sup>[a]</sup> Colan E. Hughes,<sup>[a]</sup> P. Andrew Williams,<sup>[a]</sup> Andrew J. Logsdail,<sup>[a]</sup> Yael Diskin-Posner,<sup>[b]</sup> Kenneth D. M. Harris\*<sup>[a]</sup>

**Abstract:** A new polymorph of L-tryptophan has been prepared by crystallization from the gas phase, with structure determination carried out directly from powder XRD data augmented by periodic DFT-D calculations. The new polymorph (denoted  $\beta$ ) and the previously reported polymorph (denoted  $\alpha$ ) are both based on alternating hydrophilic and hydrophobic layers, but with substantially different hydrogen-bonding arrangements. The  $\beta$  polymorph exhibits the energetically favourable L2-L2 hydrogen-bonding arrangement, which is unprecedented for amino acids with aromatic side-chains; the specific molecular conformations adopted in the  $\beta$  polymorph facilitate this hydrogen-bonding scheme while avoiding steric conflict of the side-chains.

Polymorphism arises when a molecule can exist in two or more different crystal structures.<sup>[1]</sup> As a consequence, polymorphs differ in their physicochemical properties and relative thermodynamic stabilities. From a fundamental perspective, polymorphism provides an opportunity to explore fundamental issues concerning the relationships between structure and properties of molecular solids. From an applied perspective, it is crucial to identify and characterize the range of polymorphs available to a given molecule, and to utilize the optimal polymorph in specific materials applications. As such, polymorphism plays an important role in many industrial fields including pharmaceuticals, pigments and explosives industries.

As amino acids play important roles in biological systems, there is significant interest in the structural properties of this family of materials. All 20 directly encoded proteinogenic amino acids have now had a crystal structure determined, following recently reported structures of L-arginine,<sup>[2]</sup> L-tryptophan<sup>[3]</sup> and L-lysine.<sup>[4]</sup> However, structurally characterized polymorphs have so far been reported only for L-cysteine,<sup>[5]</sup> L-glutamic acid,<sup>[6]</sup> glycine,<sup>[7]</sup> L-histidine,<sup>[8]</sup> L-isoleucine,<sup>[9]</sup> L-leucine,<sup>[10]</sup> L-phenylalanine,<sup>[11]</sup> L-proline<sup>[12]</sup> and L-serine.<sup>[13]</sup> Here we focus on L-tryptophan (L-Trp; Figure 1), for which only one crystal structure has been reported previously,<sup>[3]</sup> a remarkably complex structure containing 16 independent molecules in the asymmetric unit, with space group  $P1$ .

While crystallization from solution is the most common approach for preparing crystalline phases of organic materials (and presents wide-ranging opportunities for the discovery of

new polymorphs by varying experimental conditions, such as the choice of solvent), another method that may produce new polymorphs is crystallization from the gas phase (following sublimation). Evidence has been reported<sup>[14]</sup> for the formation of a new solid form using this strategy for crystallization of L-Trp, although the crystal structure was not determined.

Here we report the structural properties of a new polymorph of L-Trp prepared by crystallization from the gas phase. As the material is a microcrystalline powder, structure determination was carried out directly from powder XRD data.<sup>[15]</sup> We designate the new polymorph as the  $\beta$  polymorph and the previously reported polymorph<sup>[3]</sup> as the  $\alpha$  polymorph.

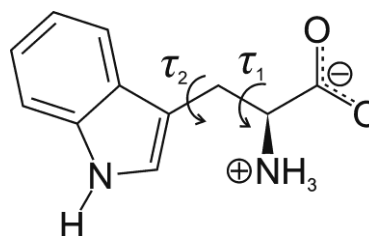


**Figure 1.** Molecular structure of L-tryptophan (torsion angles  $\tau_1$  and  $\tau_2$  are discussed in the text).

Powder XRD analysis (experimental details are in Supporting Information) of samples of L-Trp produced by crystallization from the gas phase were found to be a new polymorph<sup>[16]</sup> (designated as the  $\beta$  polymorph), with a small amount of the  $\alpha$  polymorph also present.<sup>[17]</sup> The sample deposited on the outer glass tube of the sublimation apparatus (Figure S1 in SI) contained a lower proportion of the  $\alpha$  polymorph than the sample deposited on the cold finger and was used to record high-quality powder XRD data (at ambient temperature) for structure determination.

The powder XRD pattern of the  $\beta$  polymorph was indexed using DICVOL91<sup>[18]</sup> within the CRYSFIRE package,<sup>[19]</sup> giving the following unit cell with monoclinic metric symmetry:  $a = 9.63 \text{ \AA}$ ,  $b = 5.21 \text{ \AA}$ ,  $c = 19.79 \text{ \AA}$ ,  $\beta = 94.0^\circ$ ,  $V = 990.4 \text{ \AA}^3$ . Profile fitting and unit cell refinement were carried out using the Le Bail method<sup>[20]</sup> in the program GSAS.<sup>[21]</sup> From systematic absences, the space group was assigned as  $P2_1$  (note that L-Trp must have a chiral space group). Density considerations suggest that there are four molecules of L-Trp in the unit cell and thus the asymmetric unit contains two molecules. The high-resolution solid-state  $^{13}\text{C}$  NMR spectrum recorded (Figure S2) for the same sample has two peaks in the region *ca.* 180 ppm ( $\text{CO}_2^-$  group) and two peaks in the region *ca.* 55 ppm ( $\text{CH}_2$  group), consistent with our assignment that there are two molecules of L-Trp in the asymmetric unit. Profile fitting gave a good-quality fit to the powder XRD data ( $R_{wp} = 0.73\%$ ,  $R_p = 0.54\%$ ; Figure S3), with significant discrepancies arising only due to peaks from the small amount of the  $\alpha$  polymorph present in the sample.

Structure solution was carried out using the direct-space strategy,<sup>[15a]</sup> implemented using a genetic algorithm (GA) in the program EAGER.<sup>[15b,22]</sup> In the structure solution calculations, one

[a] O. Al Rahal, Dr C. E. Hughes, Dr P. A. Williams, Dr A. J. Logsdail, Prof. K. D. M. Harris  
School of Chemistry, Cardiff University, Park Place  
Cardiff, Wales, CF10 3AT, U.K.  
E-mail: [HarrisKDM@cardiff.ac.uk](mailto:HarrisKDM@cardiff.ac.uk)

[b] Dr Y. Diskin-Posner  
Department of Chemical Research Support  
Weizmann Institute of Science  
Rehovot, 76100, Israel

<sup>‡</sup> In memory of Professor Joel Bernstein (1941-2019), an inspirational pioneer in the field of polymorphism.

of the two molecules in the asymmetric unit was defined by 8 structural variables (2 positional, 3 orientational and 3 torsional variables; for  $P2_1$ , the position of one molecule along the  $b$ -axis may be fixed) and the other molecule was defined by 9 structural variables (3 positional, 3 orientational and 3 torsional variables). Standard bond lengths and bond angles were taken from the Cambridge Structural Database using MOGUL;<sup>[23]</sup> bond lengths involving hydrogen atoms were taken from Allen *et al.*<sup>[24]</sup> Each GA calculation involved the evolution of a population of 100 trial structures and was run for 200 generations. In each generation, 10 mating operations and 50 mutation operations were applied.

In total, 40 independent GA calculations were carried out, with 29 calculations producing essentially the same structure giving the best fit to the experimental powder XRD data (i.e., with lowest  $R_{wp}$ ). This trial structure was used as the initial structure for Rietveld refinement.<sup>[25]</sup> Standard restraints were applied to bond lengths and bond angles, and planar restraints were used for the carboxylate groups and indole rings. A common isotropic displacement parameter was refined for all non-hydrogen atoms; the value for hydrogen atoms was set at 1.2 times this value. The initial Rietveld refinement produced a good fit ( $R_{wp} = 0.94\%$ ,  $R_p = 0.67\%$ ) although two hydrogen atoms in one molecule were unacceptably close, which was resolved by carrying out a periodic DFT-D energy-minimization calculation (with fixed unit cell). The structure following energy minimization was close to the structure from the initial Rietveld refinement (RMSD = 0.36 Å for non-hydrogen atoms) and was used as the initial model for further Rietveld refinement, with additional intermolecular distance restraints applied to preserve the hydrogen-bonding geometry found in the energy-minimized structure. The final Rietveld refinement (Figure 2) produced a high-quality fit ( $R_{wp} = 0.82\%$ ,  $R_p = 0.61\%$ ), comparable to the quality of fit obtained in profile fitting (Figure S3), with the following refined parameters:  $a = 9.60851(28)$  Å,  $b = 5.20198(14)$  Å,  $c = 19.7511(6)$  Å,  $\beta = 93.9514(33)^\circ$ ,  $V = 984.88(6)$  Å<sup>3</sup>. The main discrepancies in the Rietveld refinement (see the difference profile in Figure 2) arise from peaks due to the impurity of the  $\alpha$  polymorph.<sup>[26]</sup> The high-resolution solid-state <sup>13</sup>C NMR spectrum calculated (using the strategy described previously<sup>[27]</sup>) for the final refined structure is in good agreement with the experimental solid-state <sup>13</sup>C NMR spectrum (Figure S2).

The crystal structure of the  $\beta$  polymorph (Figure 3) is layered, with alternating hydrophilic and hydrophobic regions, in common with several other amino acids. The two independent molecules in the asymmetric unit have different conformations which are described as *trans* ( $\tau_1 = 179.4^\circ$ ) and *gauche* ( $\tau_1 = 52.1^\circ$ ), based on the N–C $\alpha$ –C $\beta$ –C $\gamma$  torsion angle ( $\tau_1$ ; defined in Figure 1).

The hydrophilic layer comprises two hydrogen-bonded sheets (each sheet is parallel to the  $ab$ -plane), related to each other by the  $2_1$  screw axis along the  $b$ -axis. As shown in Figure 4, a given sheet is constructed from three types of cyclic N–H $\cdots$ O hydrogen bonded array, described as  $R_4^3(14)$ ,  $R_4^4(16)$  and  $R_1^2(4)$  in graph set notation.<sup>[28]</sup> For each molecule, one N–H bond of the ammonium group connects adjacent sheets through an N–H $\cdots$ O hydrogen bond. The hydrophobic region in the  $\beta$  polymorph is a "bilayer" involving the indole rings of L-Trp molecules (Figure 3). Within one layer of the bilayer, the indole rings of the *trans* and *gauche* molecules form a nearly perpendicular arrangement, as shown in Figure S4.

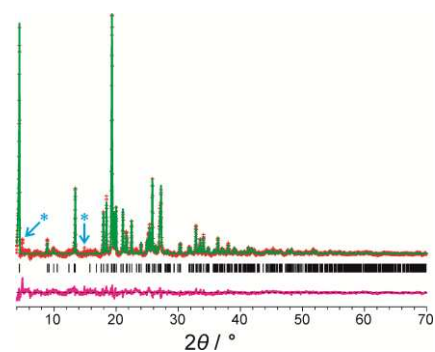


**Figure 2.** Final Rietveld refinement for the  $\beta$  polymorph of L-Trp (red crosses, experimental powder XRD pattern after background subtraction; green line, calculated powder XRD pattern; black tick marks, predicted peak positions; magenta line, difference plot). Blue asterisks indicate the main peaks due to a small impurity of the  $\alpha$  polymorph.

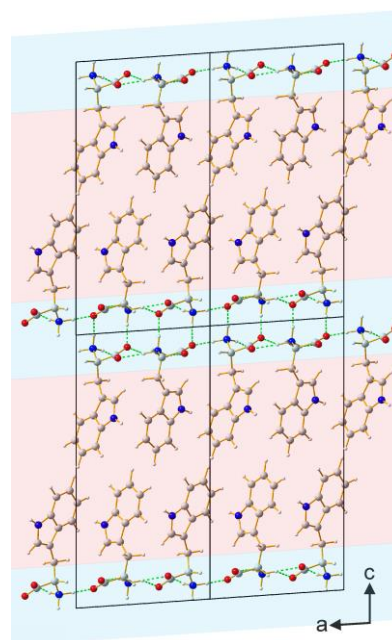


**Figure 3.** Crystal structure of the  $\beta$  polymorph of L-Trp viewed along the  $b$ -axis (hydrophilic region, cyan shading; hydrophobic region, pink shading).

According to the classification system of Görbitz *et al.*,<sup>[29]</sup> the  $\beta$  polymorph has the L2-L2 hydrogen-bonding arrangement, which is reported<sup>[29]</sup> to be the most energetically favourable hydrogen-bonding scheme for enantiopure amino acids. While the L2-L2 scheme is also reported for L-isoleucine (both polymorphs),<sup>[9]</sup> L-leucine (polymorph I),<sup>[10a]</sup> L-lysine,<sup>[4]</sup> L-methionine<sup>[30]</sup> and L-valine,<sup>[31]</sup> the  $\beta$  polymorph of L-Trp is the first case of an amino acid containing an aromatic side-chain that adopts the L2-L2 hydrogen-bonding scheme, representing a counter-example to the suggestion<sup>[29]</sup> that amino acids with aromatic side-chains cannot form this hydrogen bonding arrangement "owing to inevitable steric conflict". The conformational features that allow L-Trp to adopt the L2-L2 arrangement in the  $\beta$  polymorph by avoiding undesirable steric conflict are discussed below.

We now compare the structural properties of the  $\alpha$  and  $\beta$  polymorphs of L-Trp. Each structure comprises alternating hydrophobic and hydrophilic layers, but with significant differences in the hydrogen-bonding scheme in the hydrophilic region and in the arrangement of indole rings in the hydrophobic region. The asymmetric unit of the  $\beta$  polymorph has one *gauche* molecule and one *trans* molecule (defined by the N-C $\alpha$ -C $\beta$ -C $\gamma$  torsion angle;  $\tau_1$  in Figure 1), while the asymmetric unit of the  $\alpha$  polymorph has eight *gauche* molecules and eight *trans* molecules.<sup>[3]</sup> An important difference in molecular conformations between the  $\alpha$  and  $\beta$  polymorphs (see Figure 5) concerns the C $\alpha$ -C $\beta$ -C $\gamma$ -CH(ring) torsion angle ( $\tau_2$ ; defined in Figure 1), which defines the orientation of the indole ring relative to the amino acid head-group. For the  $\beta$  polymorph,  $\tau_2$  is relatively close to zero (*trans* molecule,  $\tau_2 = -37.5^\circ$ ; *gauche* molecule,  $\tau_2 = 8.7^\circ$ ), which means that the plane of the indole ring lies close to the C $\alpha$ -C $\beta$ -C $\gamma$  plane. In contrast, for the  $\alpha$  polymorph, the values of  $\tau_2$  are substantially larger (for *trans* molecules,  $\tau_2$  ranges from  $-112.2^\circ$  to  $-115.2^\circ$ ; for *gauche* molecules,  $\tau_2$  ranges from  $109.6^\circ$  to  $113.6^\circ$ ), such that the indole ring is tilted significantly away from the C $\alpha$ -C $\beta$ -C $\gamma$  plane.

As the C $\alpha$ -C $\beta$ -C $\gamma$  plane is essentially perpendicular to the plane of the hydrogen-bonded layer (*ab*-plane), the indole rings in the  $\beta$  polymorph project almost perpendicular to the hydrogen-bonded layer, allowing efficient packing of L-Trp molecules in the *ab*-plane and facilitating the formation of the L2-L2 hydrogen-bonding arrangement without unfavourable steric conflict. As a consequence, the area per molecule in the *ab*-plane is significantly lower for the  $\beta$  polymorph than the  $\alpha$  polymorph (Table 1) and the “thickness” of the hydrophobic bilayer is larger for the  $\beta$  polymorph (Table 1).

The relative stabilities of the  $\alpha$  and  $\beta$  polymorphs have been assessed, at 123 K and at ambient temperature, using periodic DFT-D calculations. Initially, energy-minimization calculations with fixed unit cell<sup>[32]</sup> were carried out using PBE-TS. The energies of the resultant structures were then calculated using PBE-TS, PBE-MBD, PBE0-TS and PBE0-MBD. Among these methods, PBE0-MBD is considered<sup>[33,34]</sup> to give the most reliable assessment of the relative energies of polymorphs of organic materials. From the PBE0-MBD results, the calculated energy (Table 1) is lower for the  $\beta$  polymorph by  $1.1 \text{ kJ mol}^{-1}$  at ambient temperature and by  $0.3 \text{ kJ mol}^{-1}$  at 123 K. These results suggest that the  $\beta$  polymorph may be more stable than the  $\alpha$  polymorph (although we note that the differences in energy are comparable to the errors inherent in the computational approach used, including the neglect of entropic factors). Furthermore, the  $\beta$  polymorph has higher density (Table 1) than the  $\alpha$  polymorph (by 2.8% at 123 K and 3.5% at ambient temperature), indicating that the  $\beta$  polymorph has the more efficient packing arrangement.

To investigate the possible occurrence of polymorphic phase transitions, powder XRD data were recorded on beamline I11 at Diamond Light Source for a sample of the  $\beta$  polymorph containing a small amount of the  $\alpha$  polymorph, with data recorded (Figure S5) on cooling from 290 K to 123 K and then on heating from 123 K to 440 K. Throughout this temperature cycle, no changes were observed in the relative intensities of the powder XRD patterns due to the  $\alpha$  and  $\beta$  polymorphs, and thus there is no evidence for any polymorphic transformations in this temperature range.

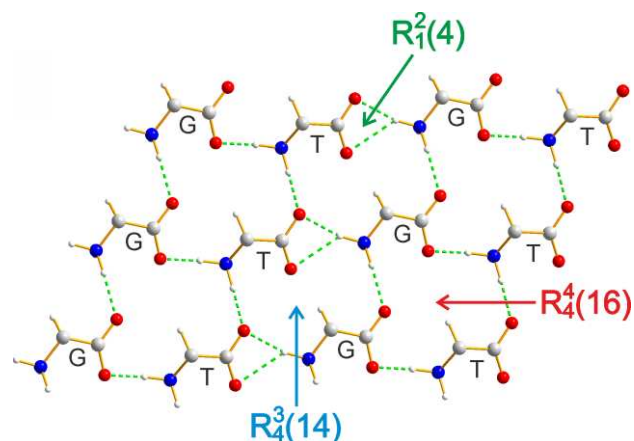


**Figure 4.** Hydrogen-bonding arrangement in a single sheet of the hydrophilic region in the  $\beta$  polymorph of L-Trp (*gauche* and *trans* molecules are labelled G and T respectively). The indole rings are omitted for clarity.

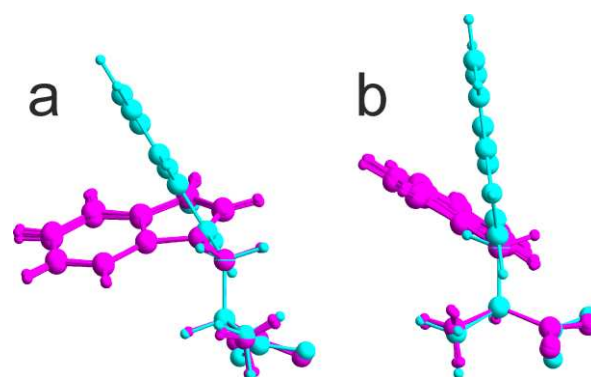


**Figure 5.** Overlays of (a) the 8 *trans* molecules in the  $\alpha$  polymorph (magenta) and the *trans* molecule in the  $\beta$  polymorph (cyan), (b) the 8 *gauche* molecules in the  $\alpha$  polymorph (magenta) and the *gauche* molecule in the  $\beta$  polymorph (cyan). The N, Ca and C $\beta$  atoms of the head-group are superimposed.

**Table 1.** Properties of the  $\alpha$  and  $\beta$  polymorphs of L-Trp at 123 K and at ambient temperature. Energies from periodic DFT-D calculations are given relative to the  $\alpha$  polymorph at 123 K. Density is calculated from the experimental unit cell volume (Table S1) and the number of molecules in the unit cell. The area per molecule in the hydrogen-bonded layer is calculated from the geometry of the *ab*-plane. The thickness of the bilayer is estimated from the perpendicular distance between the planes of adjacent hydrophilic layers (for the  $\alpha$  polymorph, the average of the values for the two crystallographically distinct bilayers is given).

Temperature Polymorph	123 K		ambient	
	$\alpha$	$\beta$	$\alpha$	$\beta$
Energy (PBE-TS) / $\text{kJ mol}^{-1}$	0.0	-0.3	1.1	0.3
Energy (PBE-MBD) / $\text{kJ mol}^{-1}$	0.0	1.0	0.7	1.2
Energy (PBE0-TS) / $\text{kJ mol}^{-1}$	0.0	-1.2	1.6	-0.4
Energy (PBE0-MBD) / $\text{kJ mol}^{-1}$	0.0	-0.3	1.3	0.2
Density / $\text{g cm}^{-3}$	1.348	1.386	1.331	1.377
Area per molecule in the hydrogen-bonded sheet / $\text{\AA}^2$	28.40	24.88	28.63	24.99
Thickness of bilayer / $\text{\AA}$	17.72	19.67	17.80	19.70

In conclusion, the new  $\beta$  polymorph of L-Trp has been prepared by crystallization from the gas phase. The crystal structure of the  $\beta$  polymorph, determined directly from powder XRD data, represents the first example of an amino acid with an aromatic side-chain that adopts the energetically favourable L2-L2 hydrogen-bonding arrangement. Periodic DFT-D calculations suggest that the  $\beta$  polymorph may be more stable than the  $\alpha$  polymorph. Finally, we emphasize the opportunity to exploit crystallization from the gas phase as a method to produce new polymorphs of other organic materials in the future (in this regard, we note that crystallization from the gas phase eliminates the solvent effects that can have a significant influence on crystallization processes from solution).

## Acknowledgements

We thank Cardiff University (PhD studentship to O. A. R.) and the Council for At-Risk Academics (Fellowship to O. A. R.) for support. We are grateful to Diamond Light Source for beam-time on powder XRD beamline I11, the U. K. High-Field Solid-State NMR Facility for spectrometer time, and the U. K. High-performance computing "Materials Chemistry Consortium" (EP/L000202) and Supercomputing Wales for access to computational facilities. We thank Prof. Chris Pickard and Prof. Martyn Guest for help and advice concerning DFT calculations.

**Keywords:** L-tryptophan • powder XRD • polymorphism • crystallization • solid-state NMR

- [1] a) J. Bernstein, *Polymorphism in Molecular Crystals*, Oxford University Press, Oxford, **2002**; b) R. J. Davey, *Chem. Commun.* **2003**, 1463-1467; c) D. Braga, F. Grepioni, *Chem. Commun.* **2005**, 3635-3645; d) S. Y. Ahn, F. Guo, B. M. Kariuki, K. D. M. Harris, *J. Am. Chem. Soc.* **2006**, *128*, 8441-8452; e) S. L. Price, *Acc. Chem. Res.* **2009**, *42*, 117-126; f) L. A. Yu, *Acc. Chem. Res.* **2010**, *43*, 1257-1266; g) P. A. Williams, C. E. Hughes, G. K. Lim, B. M. Kariuki, K. D. M. Harris, *Cryst. Growth Des.* **2012**, *12*, 3104-3113.
- [2] E. Courvoisier, P. A. Williams, G. K. Lim, C. E. Hughes, K. D. M. Harris, *Chem. Commun.* **2012**, *48*, 2761-2763.
- [3] C. H. Görbitz, K. W. Törnroos, G. M. Day, *Acta Crystallogr. Sect. B: Struct. Sci.* **2012**, *68*, 549-557.
- [4] P. A. Williams, C. E. Hughes, K. D. M. Harris, *Angew. Chem. Int. Ed.* **2015**, *54*, 3973-3977.
- [5] a) M. M. Harding, H. A. Long, *Acta Crystallogr. Sect. B: Struct. Crystallogr. Cryst. Chem.* **1968**, *24*, 1096-1102; b) K. A. Kerr, J. P. Ashmore, *Acta Crystallogr. Sect. B: Struct. Crystallogr. Cryst. Chem.* **1973**, *29*, 2124-2127; c) S. A. Moggach, D. R. Allan, S. J. Clark, M. J. Gutmann, S. Parsons, C. R. Pulham, L. Sawyer, *Acta Crystallogr. Sect. B: Struct. Sci.* **2006**, *62*, 296-309.
- [6] a) S. Hirokawa, *Acta Crystallogr.* **1955**, *8*, 637-641; b) M. S. Lehmann, A. C. Nunes, *Acta Crystallogr. Sect. B: Struct. Crystallogr. Cryst. Chem.* **1980**, *36*, 1621-1625.
- [7] a) G. Albrecht, R. B. Corey, *J. Am. Chem. Soc.* **1939**, *61*, 1087-1103; b) Y. Iitaka, *Acta Crystallogr.* **1960**, *13*, 35-45; c) Y. Iitaka, *Acta Crystallogr.* **1961**, *14*, 1-10.
- [8] a) J. J. Madden, E. L. McGandy, N. C. Seeman, *Acta Crystallogr. Sect. B: Struct. Crystallogr. Cryst. Chem.* **1972**, *B 28*, 2382-2389; b) J. J. Madden, N. C. Seeman, E. L. McGandy, *Acta Crystallogr. Sect. B: Struct. Crystallogr. Cryst. Chem.* **1972**, *B 28*, 2377-2382.
- [9] a) K. Torii, Y. Iitaka, *Acta Crystallogr. Sect. B: Struct. Crystallogr. Cryst. Chem.* **1971**, *B 27*, 2237-2246; b) S. Curland, E. Meirzadeh, Y. Diskin-Posner, *Acta Crystallogr. Sect. E: Cryst. Commun.* **2018**, *74*, 776-779.
- [10] a) M. M. Harding, R. M. Howieson, *Acta Crystallogr. Sect. B: Struct. Sci. Cryst. Eng. Mater.* **1976**, *32*, 633-634; b) M. Yamashita, S. Inomata, K. Ishikawa, T. Kashiwagi, H. Matsuo, S. Sawamura, M. Kato, *Acta Crystallogr. Sect. E: Cryst. Commun.* **2007**, *63*, O2762-O2764.
- [11] a) P. A. Williams, C. E. Hughes, A. B. M. Buanz, S. Gaisford, K. D. M. Harris, *J. Phys. Chem. C* **2013**, *117*, 12136-12145; b) F. S. Ihlefeldt, F. B. Pettersen, A. von Bonin, M. Zawadzka, C. H. Görbitz, *Angew. Chem. Int. Ed.* **2014**, *53*, 13600-13604.
- [12] a) R. L. Kayushina, B. K. Vainshtein, *Kristallografiya* **1965**, *10*, 833-844; b) N. Tumanova, N. Tumanov, K. Robeyns, F. Fischer, L. Fusaro, F. Morelle, V. Ban, G. Hautier, Y. Filinchuk, J. Wouters, T. Leyssens, F. Emmerling, *Cryst. Growth Des.* **2018**, *18*, 954-961.
- [13] a) T. J. Kistenmacher, G. A. Rand, R. E. Marsh, *Acta Crystallogr. Sect. B: Struct. Sci. Cryst. Eng. Mater.* **1974**, *30*, 2573-2578; b) S. A. Moggach, D. R. Allan, C. A. Morrison, S. Parsons, L. Sawyer, *Acta Crystallogr. Sect. B: Struct. Sci.* **2005**, *61*, 58-68; c) S. A. Moggach, W. G. Marshall, S. Parsons, *Acta Crystallogr. Sect. B: Struct. Sci.* **2006**, *62*, 815-825; d) M. Fisch, A. Lanza, E. Boldyreva, P. Macchi, N. Casati, *J. Phys. Chem. C* **2015**, *119*, 18611-18617.
- [14] Z. Liu, C. Li, *Biophys Chem* **2008**, *138*, 115-119.
- [15] a) K. D. M. Harris, M. Tremayne, P. Lightfoot, P. G. Bruce, *J. Am. Chem. Soc.* **1994**, *116*, 3543-3547; b) K. D. M. Harris, S. Habershon, E. Y. Cheung, R. L. Johnston, *Z. Kristallogr.* **2004**, *219*, 838-846; c) K. D. M. Harris, E. Y. Cheung, *Chem. Soc. Rev.* **2004**, *33*, 526-538; d) K. D. M. Harris, *Top. Curr. Chem.* **2012**, *315*, 133-177.
- [16] At this stage, it was unclear whether the material obtained was the same as the material obtained previously<sup>[14]</sup> by crystallization from the gas phase, as there are significant differences in the powder XRD data for these materials. This issue was resolved after completing the structure determination of the  $\beta$  polymorph, as discussed in SI.
- [17] Preparation of the  $\beta$  polymorph was repeated extensively in order to obtain a phase pure sample, but in all cases a small amount of the  $\alpha$  polymorph was found to be present.
- [18] A. Boulitif, D. Louër, *J. Appl. Cryst.* **1991**, *24*, 987-993.
- [19] R. Shirley, *The CRYSFIRE System for Automatic Powder Indexing: User's Manual*, The Lattice Press, Guildford, U.K., **1999**.
- [20] A. Le Bail, H. Duroy, J. L. Fourquet, *Mat. Res. Bull.* **1988**, *23*, 447-452.
- [21] A. C. Larson, R. B. Von Dreele, *Los Alamos National Laboratory Report* **2004**, LAUR 86-748.
- [22] a) B. M. Kariuki, P. Calcagno, K. D. M. Harris, D. Philp, R. L. Johnston, *Angew. Chem. Int. Ed.* **1999**, *38*, 831-835; b) B. M. Kariuki, K. Psallidas, K. D. M. Harris, R. L. Johnston, R. W. Lancaster, S. E. Staniforth, S. M. Cooper, *Chem. Commun.* **1999**, 1677-1678; c) E. Tedesco, G. W. Turner, K. D. M. Harris, R. L. Johnston, B. M. Kariuki, *Angew. Chem. Int. Ed.* **2000**, *39*, 4488-4491; d) D. Albesa-Jové, B. M. Kariuki, S. J. Kitchin, L. Grice, E. Y. Cheung, K. D. M. Harris, *ChemPhysChem* **2004**, *5*, 414-418; e) F. Guo, J. Martí-Rujas, Z. Pan, C. E. Hughes, K. D. M. Harris, *J. Phys. Chem. C* **2008**, *112*, 19793-19796; f) C. E. Hughes, G. N. M. Reddy, S. Masiero, S. P. Brown, P. A. Williams, K. D. M. Harris, *Chem. Sci.* **2017**, *8*, 3971-3979.
- [23] I. J. Bruno, J. C. Cole, M. Kessler, J. Luo, W. D. S. Motherwell, L. H. Purkis, B. R. Smith, R. Taylor, R. I. Cooper, S. E. Harris, A. G. Orpen, *J. Chem. Inf. Comput. Sci.* **2004**, *44*, 2133-2144.
- [24] F. H. Allen, O. Kennard, D. G. Watson, L. Brammer, A. G. Orpen, R. Taylor, *J. Chem. Soc. Perkin Trans. 2* **1987**, S1-S19.
- [25] H. M. Rietveld, *J. Appl. Crystallogr.* **1969**, *2*, 65-71.
- [26] Given the presence of a small amount of the  $\alpha$  polymorph in the sample, Rietveld refinement of the  $\beta$  polymorph was also attempted with the  $\alpha$  polymorph included as a second phase. However, such refinements were unstable, as discussed further in SI.
- [27] D. V. Dudenko, P. A. Williams, C. E. Hughes, O. N. Antzutkin, S. P. Velaga, S. P. Brown, K. D. M. Harris, *J. Phys. Chem. C* **2013**, *117*, 12258-12265.

- 
- [28] M. C. Etter, J. C. Macdonald, J. Bernstein, *Acta Crystallogr. Sect. B: Struct. Sci.* **1990**, *46*, 256-262.
- [29] C. H. Görbitz, K. Vestli, R. Orlando, *Acta Crystallogr. Sect. B: Struct. Sci. Cryst. Eng. Mater.* **2009**, *65*, 393-400.
- [30] K. Torii, Y. Iitaka, *Acta Crystallogr. Sect. B: Struct. Sci. Cryst. Eng. Mater.* **1973**, *29*, 2799-2807.
- [31] K. Torii, Y. Iitaka, *Acta Crystallogr. Sect. B: Struct. Crystallogr. Cryst. Chem.* **1970**, *26*, 1317-1326.
- [32] The initial structures used in the energy-minimization calculations were derived as follows: (i)  $\alpha$  polymorph at 123 K: structure from single-crystal XRD reported previously;<sup>[3]</sup> (ii)  $\beta$  polymorph at 123 K: structure determined from powder XRD in the present work (see SI); (iii)  $\alpha$  polymorph at ambient temperature: unit cell determined from single-crystal XRD in the present work (see SI) together with the fractional coordinates reported<sup>[3]</sup> for the structure at 123 K; (iv)  $\beta$  polymorph at ambient temperature: structure determined from powder XRD in the present work.
- [33] A. G. Shtukenberg, Q. Zhu, D. J. Carter, L. Vogt, J. Hoja, E. Schneider, H. Song, B. Pokroy, I. Polishchuk, A. Tkatchenko, A. R. Oganov, A. L. Rohl, M. E. Tuckerman, B. Kahr, *Chem. Sci.* **2017**, *8*, 4926-4940.
- [34] J. Hoja, H. Y. Ko, M. A. Neumann, R. Car, R. A. DiStasio, A. Tkatchenko, *Sci. Adv.* **2019**, *5*, eaau3338.
-

---

---